Pulmonary Nodules: Sensitivity of Maximum Intensity Projection versus That of Volume Rendering of 3D Multidetector CT Data[1]

Philipp Peloschek, MD
Johannes Sailer, MD
Michael Weber, MSc
Christian J. Herold, MD
Mathias Prokop, MD
Cornelia Schaefer-Prokop, MD

Purpose: To prospectively compare maximum intensity projection (MIP) and volume rendering (VR) of multidetector computed tomographic (CT) data for the detection of small intrapulmonary nodules.

Materials and Methods: This institutional review board–approved prospective study included 20 oncology patients (eight women and 12 men; mean age, 56 years ± 16 [standard deviation]) who underwent clinically indicated standard-dose thoracic multidetector CT and provided informed consent. Transverse thin slabs of the chest (thickness, 7 mm; reconstruction increment, 3.5 mm) were created by using MIP and VR techniques to reconstruct CT data (collimation, 16 × 0.75 mm) and were reviewed in interactive cine mode. Mean, minimum, and maximum reading time per examination and per radiologist was documented. Three radiologists digitally annotated all nodules seen in a way that clearly determined their locations. The maximum number of nodules detected by the three observers and confirmed by consensus served as the reference standard. Descriptive statistics were calculated, with $P < .05$ indicating a significant difference. The Wilcoxon matched-pairs signed rank test and confidence intervals for differences between methods were used to compare the sensitivities of the two methods.

Results: VR performed significantly better than MIP with regard to both detection rate ($P < .001$) and reporting time ($P < .001$). The superiority of VR was significant for all three observers and for nodules smaller than 11 mm in diameter and was pronounced for perihilar nodules ($P = .023$). Sensitivities achieved with VR ranged from 76.5% to 97.3%, depending on nodule size.

Conclusion: VR is the superior reading method compared with MIP for the detection of small solid intrapulmonary nodules.

[1] From the Department of Radiology, Vienna Medical University, Währinger Gürtel 18-20, A-1090 Vienna, Austria (P.P., J.S., M.W., C.J.H.); Department of Radiology, Utrecht Medical Center, Utrecht, the Netherlands (M.P.); and Department of Radiology, Academic Medical Center, University of Amsterdam, Amsterdam, the Netherlands (C.S.). Received December 16, 2005; revision requested February 10, 2006; revision received May 30; accepted June 20; final version accepted September 5. Supported by grant P17083-N04 from the Austrian Funds for Scientific Research. **Address correspondence to** P.P. (e-mail: *philipp.peloschek@meduniwien.ac.at*).

Most of the previous limitations inherent to single-detector computed tomographic (CT) technology have been resolved with the use of multidetector CT. However, human perception errors currently seem to be the most important limiting factor in the detection of small intrapulmonary nodules (1–9). The goal of reducing perception errors in a multitude of transverse scans has stimulated researchers to develop dedicated computer applications and advanced three-dimensional (3D) displays to assist the radiologist (5,10–17).

Maximum intensity projection (MIP) and volume rendering (VR) represent two commercially available techniques for displaying a subvolume of the 3D data set. Results of previous studies (13,18,19) have already proved the superiority of MIP over the reading of transverse sections for the detection of pulmonary nodules. The VR technique represents a more advanced 3D volume reconstruction method that is based on the assignment of opacity values to CT numbers: High opacity values produce an appearance similar to surface rendering, and low opacity values allow the user to "see through" structures. MIP is confined to the display of voxels with the maximum intensity found along a projection line from the viewer's eye through the 3D volume of interest (3,13,18–20). In addition, VR leads to an apparent enlargement of structures with an absorption higher than that of the surrounding tissues, depending on the opacity values applied.

We hypothesized that transverse thin-slab VR would be more sensitive in the detection of intrapulmonary nodules than MIP by improving the spatial orientation of the reporting radiologist and virtually increasing the size of pulmonary nodules. Thus, the purpose of our study was to prospectively compare MIP and VR for the detection of small intrapulmonary nodules at multidetector CT.

Advances in Knowledge

- Pulmonary nodules were seen by more readers at multidetector CT when volume rendering (VR) was used than when maximum intensity projection (MIP) was used ($P < .001$).
- VR performed significantly better than MIP for nodules smaller than 11 mm in diameter ($P < .001$) and equivalent to MIP ($P = .061$) for larger nodules.
- The superiority of VR to MIP was evident for perihilar nodules.
- The number of nodules that were smaller than 11 mm and found exclusively with VR was significantly higher ($P < .02$) than the number of nodules of this size seen exclusively with MIP; this difference did not reach significance for larger nodules.
- Interobserver agreement was higher with VR than with MIP and reached significance for two of the three reader pairs ($P < .001$).

Materials and Methods

The software used was provided free of charge by Siemens Medical Solutions (Erlangen, Germany) as part of a 6-month cooperation contract for research and education. The authors had full control of the data. None of the authors is an employee of or a consultant for Siemens Medical Solutions.

Patients and Nodule Distribution

We performed a prospective analysis of clinically indicated CT data. All 65 patients (37 men and 28 women; mean age, 62 years ± 21 [standard deviation]; age range, 35–87 years) included in the study underwent chest CT for clinical indications. Reasons for referral included detection of metastasis, as well as follow-up of known pulmonary metastasis. The study protocol was approved by the internal review board (ethics committee) of the Vienna Medical University, and written informed consent was obtained from all patients.

Patient inclusion was determined by a chest radiologist who was not involved in the reading process (M.P., with 15 years of experience in thoracic imaging). Patient inclusion was not consecutive owing to the application of exclusion criteria (Fig 1); patients were selectively included in the study group if CT showed between one and 20 intrapulmonary nodules that were smaller than 2 cm in diameter. We aimed for a sample size of between 160 and 180 nodules, as was suggested before the study by the results of a power analysis (nQuery Adviser, version 5.0; Statistical Solutions, Cork, Ireland), to ensure a power of 80% for detecting a medium effect size of $\varepsilon = .5$ at a significance level of $P < .05$, according to Cohen (21). Therefore, patient inclusion was terminated when more than 160 isolated intrapulmonary nodules had been detected.

Data sets without isolated intrapulmonary nodules and data sets with more than 20 nodules were excluded, as well as data sets that showed coexisting pulmonary abnormalities such as extensive scarring, pneumonia, fibrosis, or edema.

Finally, eight women and 12 men (mean age, 56 years ± 16; age range, 35–71 years) were included; the total number of isolated intrapulmonary nodules, as detected by three observers and confirmed by consensus, was 163. Four of the 20 patients had up to two nodules, 10 patients had between three and 10 nodules, and six patients had between 10 and 20 nodules. The distribution of lesions with regard to size was as follows: 51 (31.3%) of the 163 nodules were 5 mm or smaller, 75 (46.0%) were

Published online
10.1148/radiol.2432052052

Radiology 2007; 243:561–569

Abbreviations:
MIP = maximum intensity projection
3D = three-dimensional
VR = volume rendering

Author contributions:
Guarantor of integrity of entire study, P.P.; study concepts/study design or data acquisition or data analysis/interpretation, all authors; manuscript drafting or manuscript revision for important intellectual content, all authors; manuscript final version approval, all authors; literature research, P.P., C.J.H., M.P.; clinical studies, P.P., J.S., C.S.; statistical analysis, P.P., J.S., M.W., M.P., C.S.; and manuscript editing, all authors

See Materials and Methods for pertinent disclosures.

between 6 and 10 mm, and 37 (22.7%) were larger than 10 mm in diameter.

Nodules were grouped according to their location by one of the authors who was not involved in the reading process (M.P). Nodules classified as perihilar were located in a 2-cm zone around the hilum; peripheral nodules were defined as those within 1 cm of the pleural surface, including the space along the cardiomediastinal silhouette; and the remaining nodules located in the core of the parenchyma were classified as central. The final distribution included 39 (24%) perihilar nodules, 67 (41%) peripheral nodules, and 35 (35%) central nodules. This distribution of nodules was similar to data reported in previous studies (5,13).

Technical Parameters

Images were obtained with a subsecond 16-section multidetector CT scanner (Somatom Sensation; Siemens Medical Solutions) in a single breath hold at 120 kV, 100 mAs (effective), and a collimation of 16 × 0.75 mm. Scanning was performed from the lung apices to the upper abdomen. An intravenous contrast agent (iopromide, Ultravist; Schering, Berlin, Germany) was administered (100 mL [300 mg iodine per milliliter]) with an injection rate of 4 mL/sec. Scans were acquired with a delay of 40 seconds. In our institution, we routinely administer intravenous contrast material in oncology patients known to have or suspected of having pulmonary metastases because of the resulting improved anatomic orientation in the mediastinum and interpretation of potential intrapulmonary consolidations. We did not expect contrast material use to have an effect on pulmonary nodule detection.

Thin sections (width, 1 mm) were reconstructed with a reconstruction increment of 0.75 mm by using a high-resolution reconstruction algorithm with standardized window level and width settings for the lung parenchyma (window level, −650 HU; window width, 1500 HU). Scanning length varied between 30 and 35 cm and resulted in 300–350 transverse images per patient.

Three-dimensional Transverse Thin-Slab Reconstructions

The 20 data sets included in the study group were sent to a dedicated workstation (Leonardo; Siemens Medical Solutions) with software (Syngo LungCare; Siemens Medical Solutions). This software allows the real-time 3D processing of sliding thin-slab MIP and VR reconstructions without user interaction.

Thin-slab 7-mm-thick MIPs were reconstructed from the 1-mm transverse sections; MIP slabs were reconstructed at an increment of 3.5 mm. Thin-slab VR images with a 7-mm section thickness and a 3.5-mm reconstruction increment were also reconstructed from the 1-mm transverse sections. In our study, 50% opacity was set at −400 HU, and voxels with an attenuation of 200 HU or greater were assigned 100% opacity.

Image Interpretation

Data sets were reviewed at the dedicated workstation by using the commercially available software, which allowed for real-time reconstruction and cine-mode display of thin-slab VR and MIP images. Three radiologists independently analyzed the MIP and VR data sets. Observers A and C (J.S. and P.P., each with 5 years of experience) were trained in general body imaging, and observer B (C.S., with 15 years of experience) was specialized in thoracic imaging.

All observers were familiar with the appearance of MIP and VR images and with the workstation used. Studies were randomly presented with regard to patient order and to the order of the technique used (MIP or VR). No observer saw both MIP and VR images in a particular patient within the same reading session. To avoid memory effects, we ensured that at least 4 weeks elapsed between reading sessions.

An isolated intrapulmonary nodule was defined as a round opacity completely surrounded by lung with a ratio of less than 2 between its maximum and minimum diameter (19).

Criteria and methods for reporting had been defined before the study, and observers were trained before study initiation by evaluating a training data set obtained in five additional patients with a total of 37 intrapulmonary nodules that were not included in the final data analysis.

Observers were not informed about the number of lesions per patient and were asked to annotate each nodule they saw in a way that clearly determined its location.

Statistical Analysis

Our study lacked an absolute standard of truth because histopathologic proof was not available, and we are aware of no other imaging method that provides performance superior to CT for the detection of intrapulmonary nodules. We therefore aimed to compare the sensitivities of the two 3D techniques rather than to determine absolute sensitivity. The maximum number of nodules detected by all three readers and confirmed by consensus served as the reference standard. We further classified the nodules into three subcategories according to their size and location, as described above. We also documented the mean, minimum, and maximum reading time per examination and per radiologist.

Statistical analysis was performed with software (SPSS for Windows, version 11.5.1, SPSS, Chicago, Ill; EGRET, version 2.0.31, Cytel Software Corporation, Cambridge, Mass). The significance level was set at $P < .05$.

The following tests were performed:

1. First, we calculated the sensitivity of the two 3D techniques on a nodule-

Figure 1

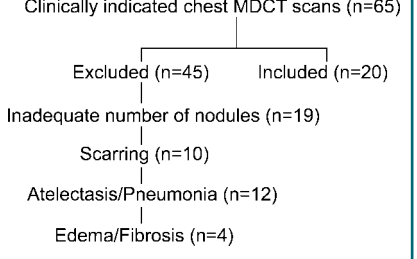

Figure 1: Flowchart of patient inclusion. *MDCT* = multidetector CT.

by-nodule basis: A Wilcoxon matched-pairs signed rank test assessed nodule by nodule whether the number of observers who had detected that nodule significantly differed between the two 3D modes. In this test, the nodule size was the dependent variable and the 3D mode was the independent variable. The significance level was set at $P < .05$. A two-way analysis was performed to also consider the influence of nodule location. In that test, the nodule size was the dependent variable and nodule location and 3D technique were the independent variables.

2. We then calculated the sensitivity of the two 3D techniques on a reader-by-reader basis. A significant difference was indicated when zero was not included within the bounds of the 95% confidence intervals.

3. We applied the McNemar test to determine whether one 3D technique yielded a significantly higher number of nodules that were seen exclusively with that 3D technique.

4. In addition, a logistic regression analysis with random effects was performed for each reader separately to compare the sensitivity of the two methods, taking multiple nodules per patient into account.

5. Interobserver agreement was determined in a pairwise fashion by comparing observers A and B, observers B and C, and observers A and C in turn. The significance of differences was tested by calculating the 95% confidence intervals.

6. The efficiency of the two 3D techniques, with regard to required reading time, was determined by calculating the mean, minimum, and maximum time needed to read the examinations. Reading times were averaged over the three observers for MIP and VR. Data were compared with a two-way analysis of variance with repeated measures, with time being the dependent variable and readers and viewing technique being the independent variables.

Table 1

Results of Wilcoxon Matched-Pairs Signed Rank Test to Compare Number of Correct Annotations of 163 Nodules on Nodule-by-Nodule Basis

Parameter	No. of Nodules	Mean Rank
Nodules identified by more readers with MIPs than with VR images	12	36.50
Nodules identified by more readers with VR images than with MIPs	71	42.93
Ties	80	. . .

Note.—The use of VR images resulted in a higher number of correct annotations in a significantly larger number of nodules ($P < .001$; z score, −6.125) than did the use of MIPs.

Table 2

Results of Wilcoxon Matched-Pairs Signed Rank Test to Compare Number of Correct Annotations of 163 Nodules on Nodule-by-Nodule Basis according to Different Nodule Sizes

Parameter	No. of Nodules	Mean Rank
	Nodules 5 mm or Smaller*	
Nodules identified by more readers with MIPs than with VR images	6	12.50
Nodules identified by more readers with VR images than with MIPs	27	18.00
Ties	18	. . .
	6–10-mm Nodules†	
Nodules identified by more readers with MIPs than with VR images	5	17.00
Nodules identified by more readers with VR images than with MIPs	35	21.00
Ties	35	. . .
	11–20-mm Nodules‡	
Nodules identified by more readers with MIPs than with VR images	1	8.50
Nodules identified by more readers with VR images than with MIPs	9	5.17
Ties	27	. . .

* VR images enabled significantly better performance ($P < .001$; z score, −3.776) than did MIPs for nodules of this size range.

† VR images enabled significantly better performance ($P < .001$; z score, −4.699) than did MIPs for nodules of this size range.

‡ The difference in performance with the two kinds of images did not reach significance ($P = .061$; z score, −2.013) for nodules of this size range.

Results

Sensitivity of MIP versus VR on Nodule-by-Nodule Basis

On a nodule-by-nodule basis, nodules were seen by more readers with VR than with MIP. Results of the Wilcoxon matched-pairs signed rank test indicated that VR was superior to MIP at $P < .001$ (Table 1). With regard to nodule diameter, the Wilcoxon matched-pairs signed rank test revealed a significantly superior performance for VR over MIP for nodules 5 mm or smaller and for nodules between 6 and 10 mm in diameter (Table 2), but not for nodules between 11 and 20 mm. There was a significant interaction ($P = .023$) between nodule location and 3D technique. The difference in performance was more evident for the perihilar nodules, as indicated in Figures 2 and 3.

Sensitivity of MIP versus VR on Reader-by-Reader Basis

All three observers identified more nodules with VR than with MIP (Table 3).

Figure 2

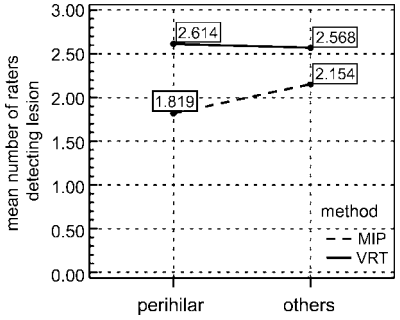

Figure 2: Graph shows mean number of readers with correct annotations averaged over different nodule location groups: VR *(VRT)* is superior to MIP regardless of nodule location. Differences are most pronounced for perihilar nodules.

Figure 3

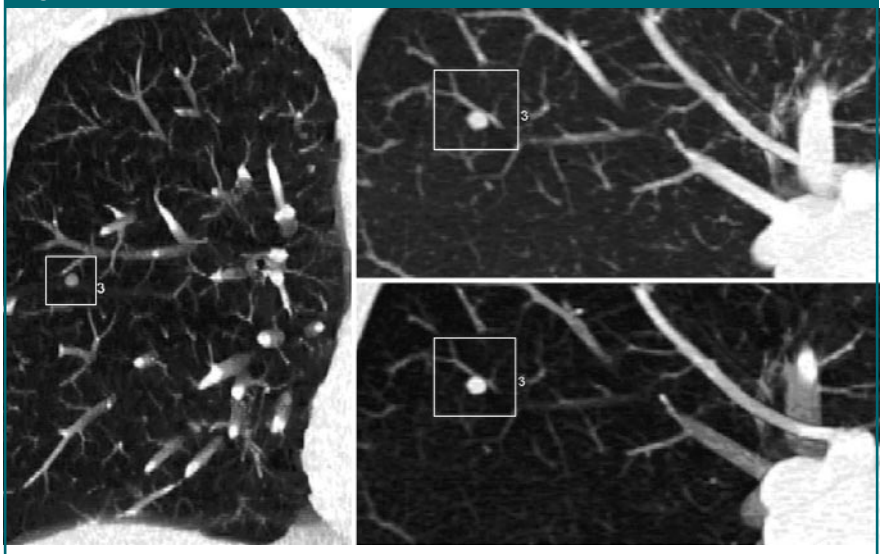

Figure 3: Coronal VR (left), transverse MIP (top right), and transverse VR (bottom right) of CT data set in 65-year-old patient with metastatic melanoma. VR images display vessels and the nodule with different densities such that spatial allocation is preserved and the distracting influence of "anatomic noise" is reduced. In the MIP image, however, vascular structures and the nodule have the same attenuation, making it more difficult to visually differentiate between anatomic structures and focal disease.

For all three observers, zero was not included within the boundaries of the 95% confidence intervals, indicating that the performance differences were significant for all three observers (Table 4). The number of nodules 5 mm or smaller and between 6 and 10 mm found exclusively with VR was significantly higher than the number of such nodules seen exclusively with MIP. For nodules larger than 10 mm, this difference did not reach significance (Table 5). The logistic regression analysis with random effects also revealed higher sensitivities with VR for all readers ($P < .001$).

Interobserver Agreement

Interobserver agreement was generally higher with VR than with MIP. The differences reached significance ($P = .001$) for the agreement between readers A and B and the agreement between readers B and C but not the agreement between readers A and C (Table 6).

Length of Reading Time

Reading time, averaged over the three observers, was 4.5 minutes for VR images (range, 2.2–6.8 minutes) and 5.4 minutes for MIP images (range, 2.8–8.0 minutes). This difference reached significance ($P < .001$). The three readers did not differ significantly among each other with regard to their reading times.

Table 3

Number of Pulmonary Nodules Detected by Each Observer with Each 3D Technique

Nodule Size (mm)	No. of Nodules	Observer A*		Observer B†		Observer C‡	
		MIP	VR	MIP	VR	MIP	VR
≤5	51	23 (45.1)	39 (76.5)	35 (68.6)	39 (76.5)	26 (51.0)	42 (82.4)
6–10	75	52 (69.3)	62 (82.7)	52 (69.3)	65 (86.7)	50 (66.7)	65 (86.7)
11–20	37	34 (91.9)	36 (97.3)	29 (78.4)	36 (97.3)	34 (91.9)	35 (94.6)
Total	163	109 (66.9)	137 (84.0)	116 (71.2)	140 (85.9)	110 (67.5)	142 (87.1)

Note.—Data in parentheses are sensitivity values, as percentages.

* This observer had 54 false-negative findings with the MIP technique and 26 with the VR technique.

† This observer had 47 false-negative findings with the MIP technique and 23 with the VR technique.

‡ This observer had 53 false-negative findings with the MIP technique and 21 with the VR technique.

Table 4

Sensitivity with Two 3D Techniques on Reader-by-Reader Basis according to Paired Samples Testing

Observer	Sensitivity Proportion with VR Images	Sensitivity Proportion with MIPs	Difference*
A	0.840	0.669	0.172 (0.089, 0.252)
B	0.859	0.712	0.147 (0.062, 0.231)
C	0.871	0.675	0.196 (0.111, 0.279)

Note.—For all three readers, use of VR images resulted in higher numbers.

* Data in parentheses are 95% confidence intervals. Zero is not included in any of the intervals; this indicates the differences are significant.

Table 5

Numbers of Nodules Seen Exclusively with One Method

		Observer A		Observer B		Observer C	
Nodule Size (mm)	No. of Nodules	No. of Nodules Seen Solely with MIPs	No. of Nodules Seen Solely with VR Images	No. of Nodules Seen Solely with MIPs	No. of Nodules Seen Solely with VR Images	No. of Nodules Seen Solely with MIPs	No. of Nodules Seen Solely with VR Images
≤5	51	4 (.02)	20 (.02)	7	11	5 (.03)	21 (.03)
6–10	75	6	16	6 (.02)	19 (.02)	4 (.003)	19 (.003)
11–20	37	1	3	1 (.02)	8 (.02)	2	3

Note.—Data in parentheses are *P* values.

Table 6

Interobserver Agreement with Each Technique

A: Interobserver Agreement with MIPs

	Observer		
Observer	A	B	C
A		0.6135	0.7362
B			0.6074
C			

B: Interobserver Agreement with VR Images

	Observer		
Observer	A	B	C
A		0.7853	0.7362
B			0.7790
C			

Note.—Interobserver agreement was higher with VR images than with MIPs; differences were significant ($P < .001$) for agreement between observers A and B and between observers B and C.

Discussion

Multidetector CT is the imaging technique of choice for the detection of intrapulmonary nodules. Although limitations related to spatial resolution and partial-volume effects have been overcome by multidetector CT, nodule detection is mainly limited by visual perception problems and errors (Table 7) (4,7,12,22). Reported sensitivities range from 36% to 100%, depending on nodule size and location, imaging and display parameters applied, and reader capability, and a considerable proportion of nodules remain undetected (4,5,9). Perception errors are attributable to two main factors (5). One factor is the increasing number of transverse images—owing to the use of thinner section collimation, thinner reconstruction widths, and higher volume overlap—potentially taxing the attentiveness required for accurate lung nodule identification. The second aspect that contributes to perception errors is so-called anatomic noise, which refers to the normal structures in the lung parenchyma such as vascular structures, the airways, and the interstitium.

Cine review is the first step in providing 3D information to reduce perceptual errors, and it has been shown that cine review is helpful for distinguishing nodules from obliquely oriented vessels coursing through the scanning plane. However, nodules of a size and attenuation similar to those of adjacent vessels can still quite often be overlooked (2). Since the introduction of multidetector CT, various techniques have been developed to present the 3D data volume in two-dimensional planes, conveying the spatial relationships inherent in the data with use of visual depth cues (20). The techniques differ primarily with regard to how voxels are selected and weighted. Coakley et al (18) were the first, to our knowledge, to report the use of MIP reconstructions applied to transverse images of cadaveric canine lungs. They found that use of MIP enhanced nodule detection by more than twofold compared with the use of conventional transverse images (18). Thereafter, the benefits of MIP in the detection of small lung nodules were demonstrated repeatedly under in vivo conditions as well (13,19,20).

We compared MIP and VR in our study and found a superior detection performance for VR over MIP. In addition, the number of nodules seen exclusively with one technique was higher for VR. VR techniques display the entire volume of data—not just the maximum intensity voxels—and, therefore, convey relevant information in a complex anatomic context better than MIP techniques. VR algorithms assign relative opacity values from 0% to 100% to each voxel along a line from the viewer's eye through the data set. It is noteworthy that, with VR, opacity settings have an effect on the apparent size of structures in the image: Higher opacity values make objects look larger, and lower opacity values make them look smaller (25). In our study setup, pulmonary nodules (>40 HU) were assigned high opacity values (>70%). Although the apparent increase in diameter based on the assigned opacity value may not have been of considerable magnitude, it may have contributed to the superior performance of VR.

In addition to being affected by the surrounding lung parenchyma, the detection of pulmonary nodules is also dependent on lesion properties, such as size and location. Our results indicate that VR is superior to MIP only for nodules smaller than 10 mm. For larger nodules (>10 mm), we could not find a significant performance difference, most likely due to the fact that evaluation of these lesions is less prone to visual perception errors. Nodules in a perihilar location are more difficult to detect than more peripherally located nodules owing to the close vicinity to the central vascular structures (1,13,23). Our results suggest that the superiority of VR

Table 7

Review of Publications on Detection of Pulmonary Nodules with Different CT Techniques

Authors	Publication Year	CT	Study Limitation	Suggestion
Remy-Jardin et al (7)	1993	Conventional single-detector CT	Respiratory misregistration	Spiral CT with single breath-hold technique
Mori et al (22)	1994	Single-detector CT	Section thickness	Reduce section thickness (10 mm), no influence of reconstruction algorithms
Croisille et al (23)	1995	Single-detector CT	Anatomic noise	Automated vessel subtraction and extraction
Seltzer et al (2)	1995	Single-detector CT	Large number of images, sensitivity of radiologists	Cine viewing
Coakley et al (18)	1998	Single-detector CT	Large number of images	Processing of MIP reconstructions (15 mm, 12 mm reconstruction interval)
Diederich et al (4)	1999	Single-detector CT	Partial-volume effect	Overlapping reconstruction (40%–50%)
Eibel et al (20)	2001	Four–detector row CT	Large number of images, sensitivity of radiologists	MIP is superior to transverse standard reconstructions and multiplanar reconstruction
Diederich et al (19)	2001	Single-detector CT	Projection of nodules on chest wall or vessel by MIP	Reducing MIP slab thickness to 15 mm
Kozuka et al (12)	2002	Four–detector row CT	Collimation, pitch	5-mm Collimation at pitch of 6 is sufficient, no improvement by narrowing collimation or pitch
Gruden et al (13)	2002	Four–detector row CT	Large number of images, reader fatigue, reader experience, central nodules	Processing of MIP reconstructions (10 mm, 8 mm reconstruction interval), particular benefit for detection of central nodules, and reduced effect of reader experience
Fischbach et al (24)	2003	Four–detector row CT	Section thickness	Reduce section thickness (1.25 mm)
Abe et al (10)	2004	Single-detector CT	Anatomic noise	Temporal subtraction
Wormanns et al (9)	2005	Four–detector row CT	Limited sensitivity of radiologists	Double reading
Rubin et al (5)	2005	Four–detector row CT	Limited sensitivity and high interreader variability	Double reading, computer-aided detection detects complementary pulmonary nodules

over MIP is more pronounced for perihilar nodules. This is not surprising, considering the superior capability of VR compared with MIP in demonstrating the 3D spatial relationship in the two-dimensional display.

The magnitude of sensitivities we found with MIP (45.1%–91.9%), is in accord with data published by Diederich et al (4), who reported sensitivity ranges of 36%–67% for nodules smaller than 5 mm, 72%–89% for nodules from 6 to 10 mm, and 91%–100% for lesions larger than 10 mm in diameter. The sensitivity for nodule detection with VR, however, was substantially higher in our study (76.5%–97.3%). These numbers are comparable to the detection rates achievable with double reading of transverse images, which were recently reported to amount to 74%–79% for small (size, 3.9 mm ± 3.2) pulmonary nodules (9).

We decided to evaluate 7-mm-thick slabs reconstructed with a 3.5-mm increment. Slab thickness and reconstruction increment were somewhat arbitrarily determined, driven by the goal to enable smooth cine viewing and an optimal display of lesions of interest and overlying anatomy. In contrast to previous studies (13,19), in which slabs of 10–30 mm thickness were evaluated, we used a slightly smaller slab thickness.

Further studies are warranted to evaluate the performance of VR in association or in comparison with computer-aided detection algorithms for pulmonary nodule detection. Most previous investigators assessing the effect of computer-aided detection evaluated performance differences of computer-aided detection compared with reading of transverse sections (15–17,26). Our data suggest that there is a substantially increased performance of the human visual system when 3D displays rather than transverse sections are used. Researchers who evaluate the additional benefit of computer-aided detection should consider the potentially best display technique as a reference. We found that for that specific application, VR is superior to MIP.

Average reading time with VR (4.5 minutes) was significantly shorter than with MIP (5.4 minutes). These times include the time required for digital annotation of each localized nodule, which explains the increased reporting time compared with experience in routine clinical work. The reading time did not substantially exceed the times reported in previous studies (13). The shorter reading times with VR may serve as an indirect sign of the superior spatial orientation for the readers with this technique.

The major limitation of our study was the fact that there was no absolute reference standard for the number of nodules with a method of histopathologic proof or a different, but superior, detection method. Therefore, the refer-

ence standard in this study was the maximum number of nodules detected by three readers and confirmed by consensus. Because the aim of our study was not to determine the absolute sensitivity of a particular technique but rather to compare the performance of two methods, we think that this limitation did not affect our results.

Our decision to restrict patient recruitment to only those patients referred for evaluation of possible metastatic disease represents a selection bias in favor of well-defined, solid nodules. We specifically excluded focal opacities adjacent to pleural surfaces and airways that did not meet the morphologic criteria of a round, solid lesion. We did so to minimize the discussion of what was or was not a potentially malignant nodule and accepted this limitation to achieve more constrained data in order to compare the two display techniques. Although we expected a superiority of VR over MIP for more complex focal lesions such as ground-glass nodules and nodules with irregular borders, we did not test this. We therefore must limit our conclusion to the fact that VR was superior to MIP for the depiction of solid round opacities.

Another limitation was the fact that we did not determine specificities. To determine sensitivities, we accepted the consensus of all readers as a reference standard. Because it seems even more difficult to assess the presence of potentially false-positive lesions without the presence of an absolute reference standard, we did not determine specificity values. By including only patients with one or more nodules seen on transverse images or MIPs, we missed the opportunity to find patients with one or more nodules seen exclusively on VR images, where the detection of nodules would have changed patient care. It has, however, to be noted that we focused our study solely on detection performance and did not include potential interpretative errors or effects on patient care. We also did this because our study lacks an absolute standard of histopathologic truth. From previous publications, it is known that even detected nodules may be misinterpreted if potentially abnormal features are not sufficiently recognized. This interpretation error can lead to a further increase in misdiagnosis: Of 38 missed lung cancers in a screening setting, 23 were missed owing to detection errors, and 15 were missed owing to interpretation errors (27). Because we did not aim to assess the effects on patient care, we did not include patients without a known nodule and performed a data analysis on nodule-by-nodule and reader-by-reader bases but not on a patient-by-patient basis.

Our results pertain to the particular scanning and reconstruction parameters that we used. We did not evaluate the performance of variable slab thicknesses or the effect of low-dose acquisition on VR image quality.

We conclude that VR displays are useful as an additional diagnostic review of thoracic multidetector CT data sets to highlight small solid intrapulmonary nodules in patients examined for the diagnosis of lung metastases or bronchogenic carcinoma.

References

1. Naidich DP. Volumetric scans change perceptions in thoracic CT. Diagn Imaging (San Franc) 1993;15:70–74.
2. Seltzer SE, Judy PF, Adams DF, et al. Spiral CT of the chest: comparison of cine and film-based viewing. Radiology 1995;197:73–78.
3. Napel S, Rubin GD, Jeffrey RB Jr. STS-MIP: a new reconstruction technique for CT of the chest. J Comput Assist Tomogr 1993;17:832–838.
4. Diederich S, Lentschig MG, Winter F, Roos N, Bongartz G. Detection of pulmonary nodules with overlapping vs non-overlapping image reconstruction at spiral CT. Eur Radiol 1999;9:281–286.
5. Rubin GD, Lyo JK, Paik DS, et al. Pulmonary nodules on multi-detector row CT scans: performance comparison of radiologists and computer-aided detection. Radiology 2005;234:274–283.
6. Ravenel JG, McAdams HP, Remy-Jardin M, Remy J. Multidimensional imaging of the thorax: practical applications. J Thorac Imaging 2001;16:269–281.
7. Remy-Jardin M, Remy J, Giraud F, Marquette CH. Pulmonary nodules: detection with thick-section spiral CT versus conventional CT. Radiology 1993;187:513–520.
8. Schaefer-Prokop C, Prokop M. New imaging techniques in the treatment guidelines for lung cancer. Eur Respir J Suppl 2002;35:71s–83s.
9. Wormanns D, Ludwig K, Beyer F, Heindel W, Diederich S. Detection of pulmonary nodules at multirow-detector CT: effectiveness of double reading to improve sensitivity at standard-dose and low-dose chest CT. Eur Radiol 2005;15:14–22.
10. Abe H, Ishida T, Shiraishi J, et al. Effect of temporal subtraction images on radiologists' detection of lung cancer on CT: results of the observer performance study with use of film computed tomography images. Acad Radiol 2004;11:1337–1343.
11. Armato SG 3rd, Roy AS, MacMahon H, et al. Evaluation of automated lung nodule detection on low-dose computed tomography scans from a lung cancer screening program. Acad Radiol 2005;12:337–346.
12. Kozuka T, Johkoh T, Hamada S, et al. Detection of pulmonary metastases with multi-detector row CT scans of 5-mm nominal section thickness: autopsy lung study. Radiology 2003;226:231–234.
13. Gruden JF, Ouanounou S, Tigges S, Norris SD, Klausner TS. Incremental benefit of maximum-intensity-projection images on observer detection of small pulmonary nodules revealed by multidetector CT. AJR Am J Roentgenol 2002;179:149–157.
14. Lawler LP, Wood SA, Pannu HK, Fishman EK. Computer-assisted detection of pulmonary nodules: preliminary observations using a prototype system with multidetector-row CT data sets. J Digit Imaging 2003;16:251–261.
15. Marten K, Grillhosl A, Seyfarth T, Obenauer S, Rummeny EJ, Engelke C. Computer-assisted detection of pulmonary nodules: evaluation of diagnostic performance using an expert knowledge-based detection system with variable reconstruction slice thickness settings. Eur Radiol 2005;15:203–212.
16. Kim JS, Kim JH, Cho G, Bae KT. Automated detection of pulmonary nodules on CT images: effect of section thickness and reconstruction interval—initial results. Radiology 2005;236:295–299.
17. Bae KT, Kim JS, Na YH, Kim KG, Kim JH. Pulmonary nodules: automated detection on CT images with morphologic matching algorithm—preliminary results. Radiology 2005;236:286–293.
18. Coakley FV, Cohen MD, Johnson MS, Gonin R, Hanna MP. Maximum intensity projection images in the detection of simulated pulmonary nodules by spiral CT. Br J Radiol 1998;71:135–140.

19. Diederich S, Lentschig MG, Overbeck TR, Wormanns D, Heindel W. Detection of pulmonary nodules at spiral CT: comparison of maximum intensity projection sliding slabs and single-image reporting. Eur Radiol 2001; 11:1345–1350.

20. Eibel R, Turk TR, Kulinna C, Herrmann K, Reiser MF. Multidetector-row CT of the lungs: multiplanar reconstructions and maximum intensity projections for the detection of pulmonary nodules [in German]. Rofo 2001;173:815–821.

21. Cohen J. Statistical power analysis for the behavioral sciences. Hillsdale, NJ: Lawrence Earlbaum Associates, 1988.

22. Mori K, Sasagawa M, Moriyama N. Detection of nodular lesions in the lung using helical computed tomography: comparison of fast couch speed technique with conventional computed tomography. Jpn J Clin Oncol 1994;24:252–257.

23. Croisille P, Souto M, Cova M, et al. Pulmonary nodules: improved detection with vascular segmentation and extraction with spiral CT—work in progress. Radiology 1995; 197:397–401.

24. Fischbach F, Knollmann F, Griesshaber V, Freund T, Akkol E, Felix R. Detection of pulmonary nodules by multislice computed tomography: improved detection rate with reduced slice thickness. Eur Radiol 2003;13: 2378–2383.

25. Kuszyk BS, Heath DG, Johnson PT, Eng J, Fishman EK. CT angiography with volume rendering for quantifying vascular stenoses: in vitro validation of accuracy. AJR Am J Roentgenol 1999;173:449–455.

26. Brown MS, Goldin JG, Rogers S, et al. Computer-aided lung nodule detection in CT: results of large-scale observer test. Acad Radiol 2005;12:681–686.

27. Armato SG 3rd, Li F, Giger ML, MacMahon H, Sone S, Doi K. Lung cancer: performance of automated lung nodule detection applied to cancers missed in a CT screening program. Radiology 2002;225:685–692.